IOSR Journal of Pharmacy and Biological Sciences (IOSR-JPBS)
e-ISSN:2278-3008, p-ISSN:2319-7676. Volume 18, Issue 6 Ser. 1 (Nov. – Dec. 2023), PP 61-70
www.iosrjournals.org

Pyrene induced oxidative stress and toxicity under natural light

T.S. Naqvi, Naushad Alam Shah, S.F.Mujtaba
Deptt. Of Zoology, Shia P.G. College, Lucknow

Abstract
Pyrene is one of the basic Polycyclic Aromatic hydrocarbons (PAHs) which is toxic environmental pollutant and due its presence in the environment it is being constantly exposed to natural light coming from sun. Many work is not being done on its stability under natural light and as well as its cytotoxicity. Pyrene is capable of absorbing light under 334 nm and capable of generating 1O2, O2•- and ˙OH. The intracellular ROS in HaCaT cell line was increased in concentration dependent manner in pyrene treated cells which is showed through DCF-fluorescence intensity at different concentrations of pyrene. Cell viability was reduced maximum under natural light at 1 µg/ml of pyrene. Genotoxicity was done through CPDs formation and it was maximum under UV-A at 1 µg/ml of pyrene. Mitochondrial membrane potential and its relation with DNA damage was observed after treatment with pyrene under natural light exposure. Fluorescence images of Annexin V/PI double staining, showing maximum apoptotic cells after treatment with pyrene (1 µg/ml) under natural light for a period of (30 min) exposure. The result suggest that pyrene may be cytotoxic as well as genotoxic under natural light exposure. Thus pyrene may be deleterious to human health under natural light reaching the earth surface.

I. Introduction

Polycyclic aromatic hydrocarbons (PAHs) are major pollutants in the environment formed during incomplete combustion of organic materials such as gasoline, diesel fuel, coal and oil. PAHs are a group of environmental organic pollutants that are harmful to the environment and human health. The United States Environmental Protection Agency (US-EPA) has defined 16 PAHs as priority pollutants, due to their toxicity, mutagenic and carcinogenic properties. These compounds generally with 2 to 6 condensed aromatic rings in which pyrene is one of them (Ribeiro et.al., 2012). PAHs can have major toxic effects, causing cancers in various tissues, cardiovascular disease, loss of fertility, immunosuppression and so on, in which carcinogenicity of PAHs has been well explained and accepted (Toyooka et.al., 2007). Without external stimulus PAHs are extremely stable, making them persistent environment pollutants (Samanta et.al., 2002).

Ultraviolet light (UV) is composed of UV-C, UV-B and UV-A. Most, but not all UVB is absorbed by the ozone layer hence UVB portion in sunlight is small. Maximum percentage among UV in sunlight is UVA. Due to their multiple aromatic ring system, PAHs absorb sunlight in the visible (400-700 nm) and ultraviolet (280-400 nm) of solar spectrum. Recently some PAHs listed by the U.S. Environmental Protection Agency (EPA) as priority pollutants (Yan et.al., 2004). As PAHs in the environment are usually exposed to sunlight, much more attention should be paid to the phototoxicity of PAHs. Concerning the relationship between PAHs in the environment and sunlight, photomodification of compounds, such as photodegradation and photooxidation can lead to their toxicities (Kochany and Maguire, 1994). Sunlight exposure alters anthracene (PAHs) to other forms through photodegradation (Mujtaba et.al., 2011). Photomodified Benzo(a)pyrene, Benzo(a)pyrene diones have been detected in particulate matter found in air (Teranishi et.al., 2010). The PAHs taken up in the skin can act as photosensitizers under sunlight exposure. Ultraviolet (UV) light acts as a promoter in the induction of melanomas by particular PAHs (Ingram, 1992). Benzo(a)pyrene induced the formation of γH2AX on exposure to sunlight, which resulted in double strand breakage and if not repaired properly, can result in cell death or loss of genomic integrity, eventually leading to cancer (Pierce et.al., 2001). Oxidative DNA lesions and chromosomal aberrations accumulated after treatment of primary breast cells with Benzo(a)pyrene (Sigounas et.al., 2010).

Therefore, the comparative studies on the effects of pyrene in the presence and absence of sunlight are important. The present study was carried out with human skin epidermal cell line (HaCaT) to investigate the ability of pyrene to induce oxidative stress, apoptosis and its impact on DNA damage under sunlight exposure.

II. Results

$^1O_2$ generation

Fig.1 (a) shows absorption spectra of pyrene having maximum absorption (γmax) in UV-A (334 nm). Mean photochemical generation of $^1O_2$ by pyrene (0.1 to 1 µg/ml) under sunlight (30 min), UV-A (2.16 J/cm^2) and UV-B (0.72 J/cm^2) exposures. Pyrene at 1µg/ml generates the highest amount of $^1O_2$ under sunlight followed by UV-A and UV-B exposure **(Fig. 1 b)**. In an attempt to evaluate the possible role of ROS in Pyrene phototoxicity, specific $^1O_2$ quencher was used (**Fig. 1 c**). Results showed maximum quenching of $^1O_2$ by NaN_3 (10 mM) with 1µg/ml Pyrene under UV-A (2.16 J/cm^2) exposure.

$O_2^{\bullet-}$ generation

Generation of $O_2^{\bullet-}$ is summarized in (**Fig. 2 a)**. Results showed that mean generation of $O_2^{\bullet-}$ by pyrene was comparatively higher in sunlight (30 min) followed by UV-A (2.16 J/cm^2) and UV-B (0.72 J/cm^2). The order of $O_2^{\bullet-}$ generation was following: sunlight>UV-A>UV-B. Additional evidence of the production of $O_2^{\bullet-}$ was obtained by examining the $O_2^{\bullet-}$ quenching study with SOD (10 and 25 Units/ ml) under UV-A (2.16 J/cm^2) irradiation. 80% quenching of $O_2^{\bullet-}$ was measured by 25 Units/ml of SOD (**Fig. 2 b**).

$^{\bullet}$OH generation

Generation of $^{\bullet}$OH is summarized in **(Fig. 3 a)**. Results showed that mean $^{\bullet}$OH generation was comparatively higher in sunlight (30 min) followed by UV-A (2.16 J/cm^2) and UV-B (0.72 J/cm^2). **(Fig.3 b)** shows the percent quenching of $^{\bullet}$OH under UV-A (2.16 J/cm^2) at 1µg/ml of pyrene by mannitol (0.5 M) and sodium benzoate (0.5 M) and caused 40% and 70% quenching of $^{\bullet}$OH respectively, highest quenching was observed by sodium benzoate in comparison to mannitol.

Intracellular ROS generation

Fig. 4 (a) Showed the DCF-fluorescence intensity at different concentrations of pyrene under sunlight (30 min), UV-A (2.16 J/cm^2) and UV-B (0.72 J/cm^2) exposure. As compared with control, a significant (<0.05 or p<0.01) increase in DCF intensity was observed in all treated cells in a concentration dependent manner. Maximum DCF intensity was recorded under sunlight (30 min) at 1 µg/ml of pyrene followed by UV-A and UV-B. Result indicates that pyrene facilitates UV-induced oxidative stress in HaCaT cell line. In the presence of an antioxidant, N-acetyl-cysteine (NAC) inhibited DCF fluorescence intensity in a dose-dependent manner under sunlight (30 min) exposure (**Fig. 4 b**).

Photocytotoxicity analysis

Fig. 5 (a & b) showed the pyrene phototoxicity on human keratinocyte cell line (HaCaT) through MTT and NRU assays. Photosensitizing effect of pyrene (0.1- 1 µg/ml) was recorded as percent cell viability. The phototoxicity was assessed under sunlight (30 min), UV-A (2.16 J/cm^2) and UV-B (0.72 J/cm^2) exposures. Cytotoxicity was also assessed with different pyrene concentrations without irradiation. Chlorpromazine (1 µg/ml) and L-histidine (10 µg/ml) were used as positive and negative controls, respectively. The highest decrease (p<0.01) in percent cell viability by pyrene (1 µg/ml) was observed under sunlight (80%) followed by UV-A (65%) and UV-B (50%) exposure. It indicates that UV-B irradiated pyrene (1 µg/ml) was least phototoxic, while pyrene (1 µg/ml) under sunlight was highly phototoxic. Phototoxicity of pyrene was observed in the following order: Sunlight > UV-A > UV-B. In all three exposures as concentration increase % cell viability reduced significantly (p<0.05 or p<0.01) when compared to negative control (L-Histidine). The results of MTT assay accorded the NRU assay.

Single strand breakage

The single strand breakage of DNA was measured as % tail DNA **(Fig.6 a)** and olive tail moment (OTM) **(Fig 6 b)** in the control as well as exposed cells. During electrophoresis, the cell DNA was observed to migrate more rapidly towards the anode at the highest concentration than the lowest concentration. The cell exposed to pyrene (0.1 to 1 µg/ml) under sunlight (30 min), UV-A (2.16 J/cm^2) and UV-B (0.72 J/cm^2) showed significant (p<0.05 or p<0.01) higher DNA damage than control. The gradual increase in DNA damage was observed in cells as concentration of pyrene increases and highest damage was recorded at (1 µg/ml) under sunlight followed by UV-A and UV-B irradiation.

Cyclobutane pyrimidine dimers (CPDs) formation

Pyrene (0.1 to 1 µg/ml) under sunlight/UV-R exposure induced cyclobutane pyrimidine dimers (CPDs) formation. Maximum CPDs formation were detected at1 µg/ml under sunlight (30 min) exposure. There was no significant CPDs formation under dark control cells in presence of different concentrations of pyrene (**Fig**. **7**).

Analysis of mitochondrial transmembrane potential (MMP)

Fig. 8 Mitochondrial depolarization and DNA damage were compared after treatment with pyrene (1 µg/ml) under sunlight (30 min) exposure.

The results suggest that pyrene (1 µg/ml) under sunlight exposure decreased mitochondrial membrane potential concomitantly increase in DNA damage. There was no significant decrease in mitochondrial membrane potential as well as increase in DNA damage under dark control and sunlight exposure.

Apoptosis

Our results suggest that pyrene induced apoptotic cell death under sunlight exposure. The translocation of phosphatidylserine from inner leaflet of the plasma membrane to the outer leaflet is observed early in the initiation of apoptosis without disruption of other membrane components. Using Annexin-V as specific marker for PS translocation in addition to propidium iodide, which identifies permeabilized cells. Our results suggest that photosensitized pyrene (1 µg/ml) has induced apoptosis with marked difference of early and late apoptotic cells, as compair to dark control and sunlight exposure. In presence of NAC (10 µM) photosensitized pyrene (1 µg/ml) reduced apoptotic cells significantly which advocates the involvement of ROS in pyrene phototoxicity (**Fig. 9**).

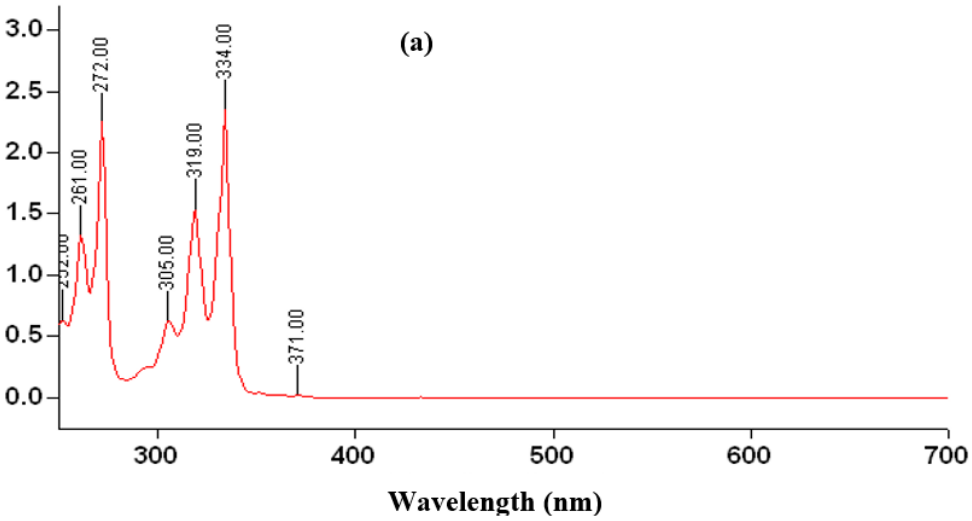

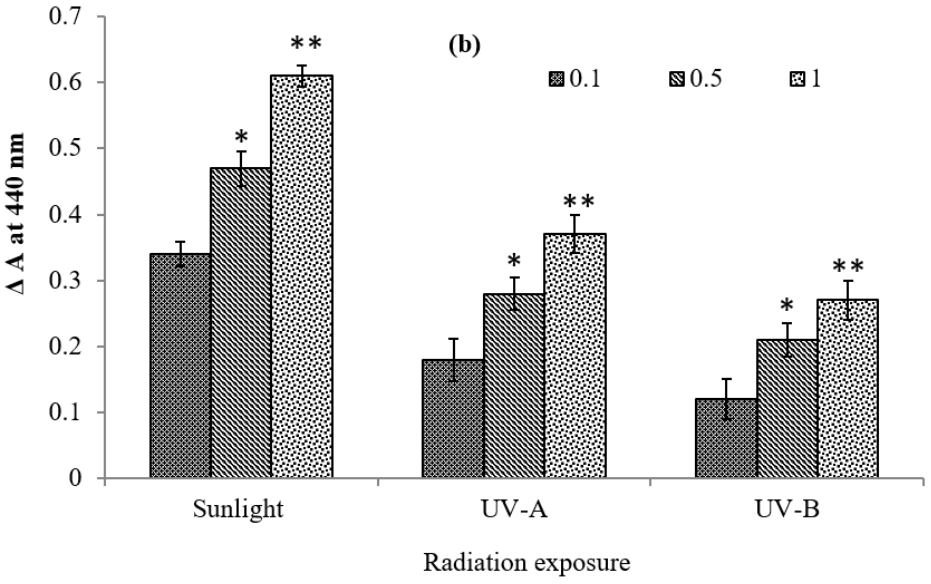

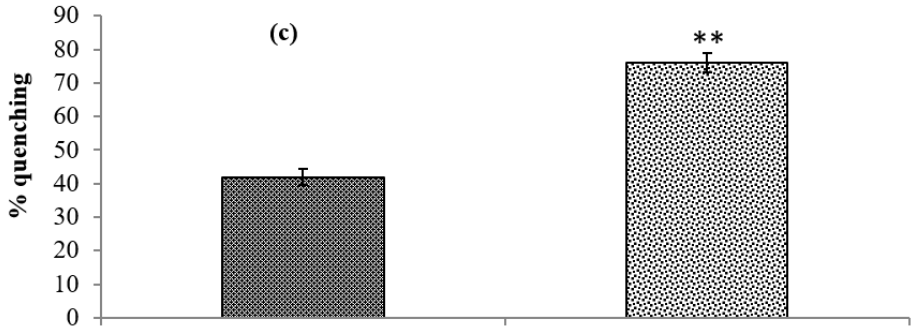

Fig. 1 (a) Absorption spectra of pyrene **(b)** Photochemical generation of $^1O_2$ by pyrene (µg/ml) at different concentrations under sunlight (30 min), UV-A (2.16 J/cm^2) and UV-B (0.72 J/cm^2) exposure. Values presented are mean of three observations ±SE. (*p<0.05 or **p<0.01- as compared to 0.1 µg/ml). **(c)** Percent photochemical quenching of $^1O_2$ generated by pyrene (1 µg/ml) through NaN_3 under UV-A (2.16 J/cm^2) exposure (**p<0.01- as compared to 5 mM NaN_3). Each value presented is mean of three observations ±SE.

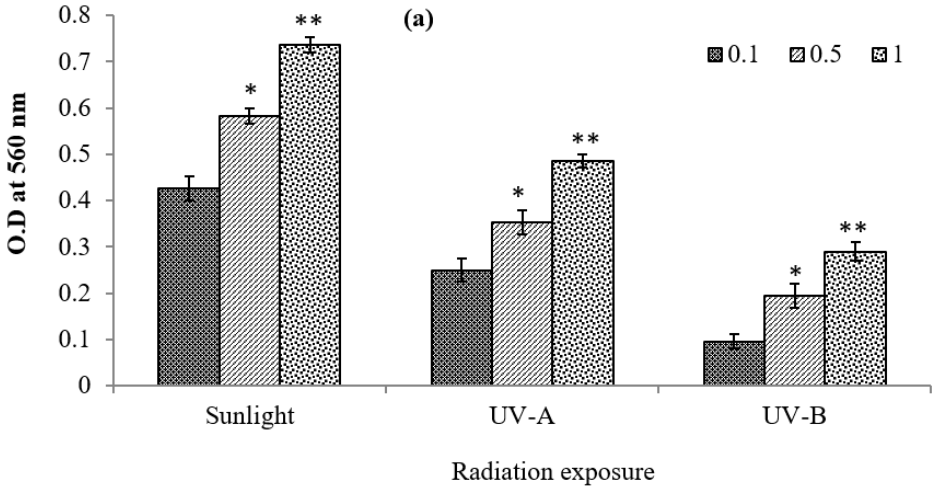

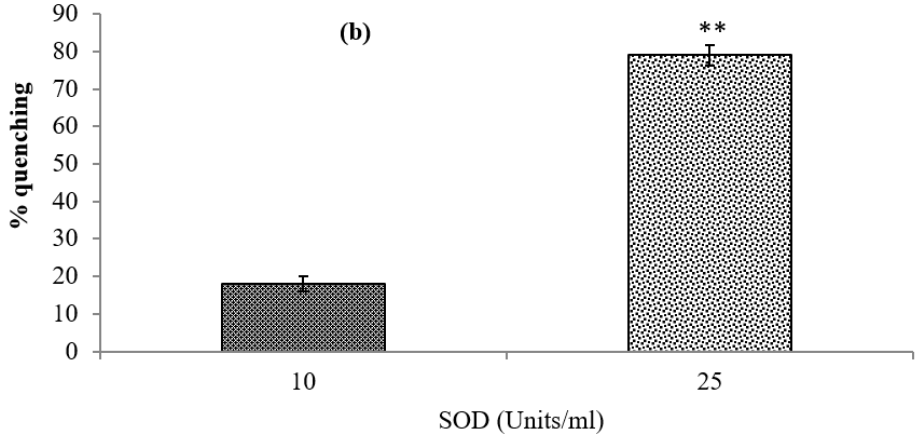

Fig. 2 (a) Photochemical generation of $O_2^{\cdot-}$ by pyrene (µg/ml) at various concentrations under Sunlight (30 min), UV-A (2.16 J/cm^2), and UV-B (0.72 J/cm^2). Values presented are mean of three observations ±SE. (*p< 0.05 or **p<0.01- as compared to 0.1 µg/ml). **(b)** Photochemical quenching of $O_2^{\cdot-}$ generated by pyrene (1 µg/ml) through SOD (10 and 25) under UV-A (2.16 J/cm^2). Values presented are mean of three observations ±SE. (**p<0.01- as compared to 10 Units/ml).

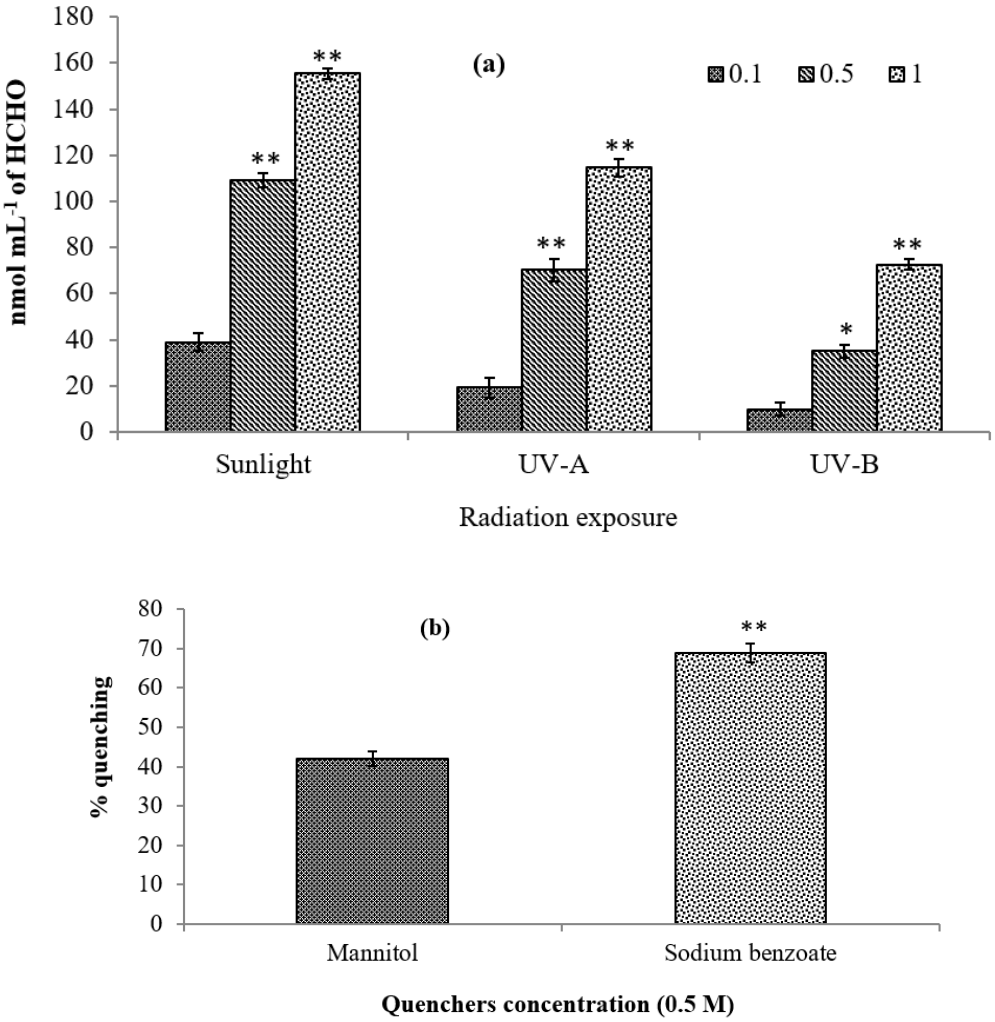

Fig. 3 (a) Photochemical generation of ·OH at various concentrations of pyrene under sunlight (30 min), UV-A (2.16 J/cm^2) and UV-B (0.72 J/cm^2). Values presented are mean of three observations ±SE. (*p<0.05 or **p<0.01- as compared to 0.1 µg/ml). **(b)** Percent quenching of ·OH at 1 µg/ml of pyrene by mannitol and sodium benzoate under UV-A (2.16 J/cm^2). Values presented are mean of three observations ±SE. (**p<0.01- as compared to 0.5 M mannitol).

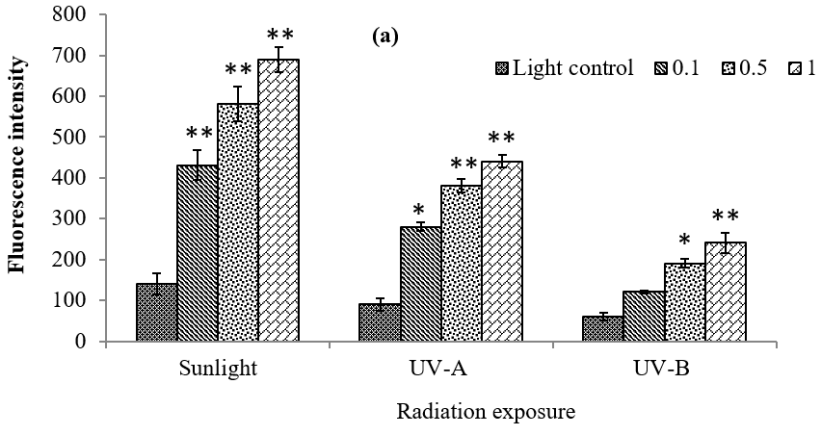

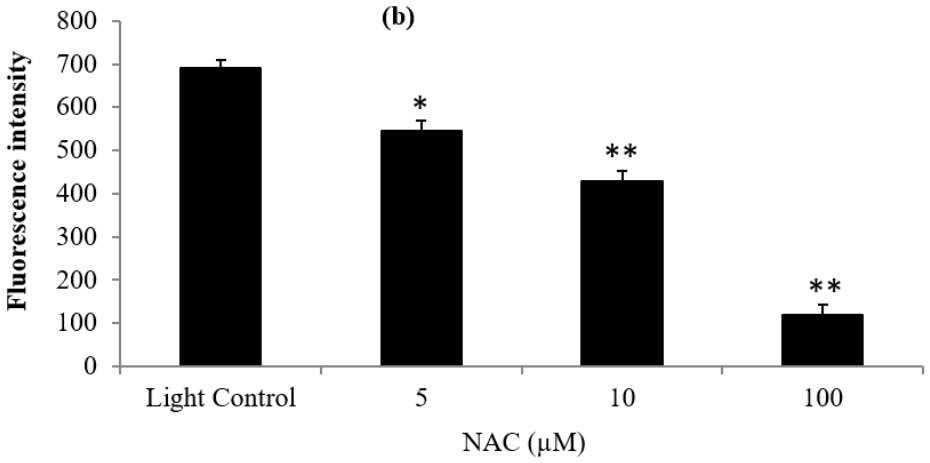

Fig. 4 (a) DCF-Fluorescence intensity at different concentrations of pyrene (µg/ml) under sunlight (30 min), UV-A (2.16 J/cm^2) and UV-B (0.72 J/cm^2) exposure. Values presented are mean of three observations ±SE. (*p<0.05 or **p<0.01- as compared to Light control). **(b)** Intracellular quenching of DCF fluorescence by NAC under sunlight (30 min) exposure. Values presented are mean of three observations ±SE. (*p<0.05 or **p<0.01- as compared to Light control).

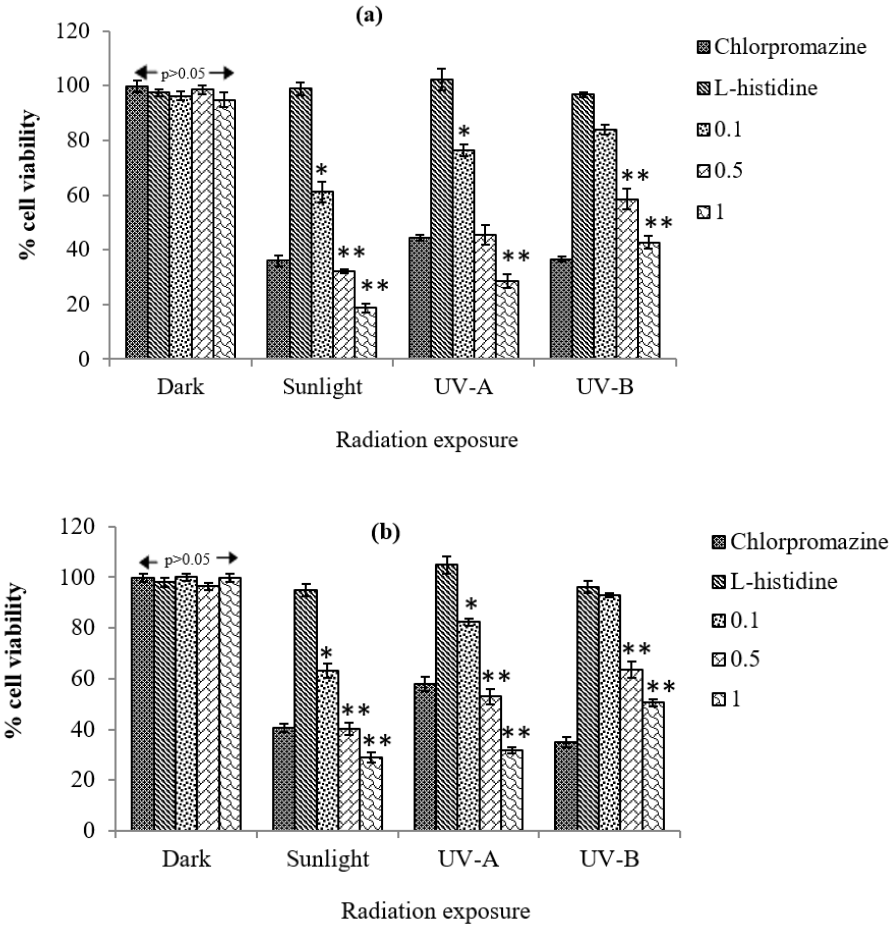

Fig. 5 Photosensitizing potential of pyrene (µg/ml) on human keratinocyte as percent cell viability by recording MTT **(a)** and NRU **(b)** assay under dark, sunlight (30 min), UV-A (2.16 J/cm^2), and UV-B (0.72 J/cm^2) exposures. Chlorpromazine (1µg/ml) and L-histidine (10 µg/ml) were used as positive and negative controls, respectively. Values presented are mean of three observations ± SE. (*p<0.05 or **p<0.01- as compared to L-Histidine).

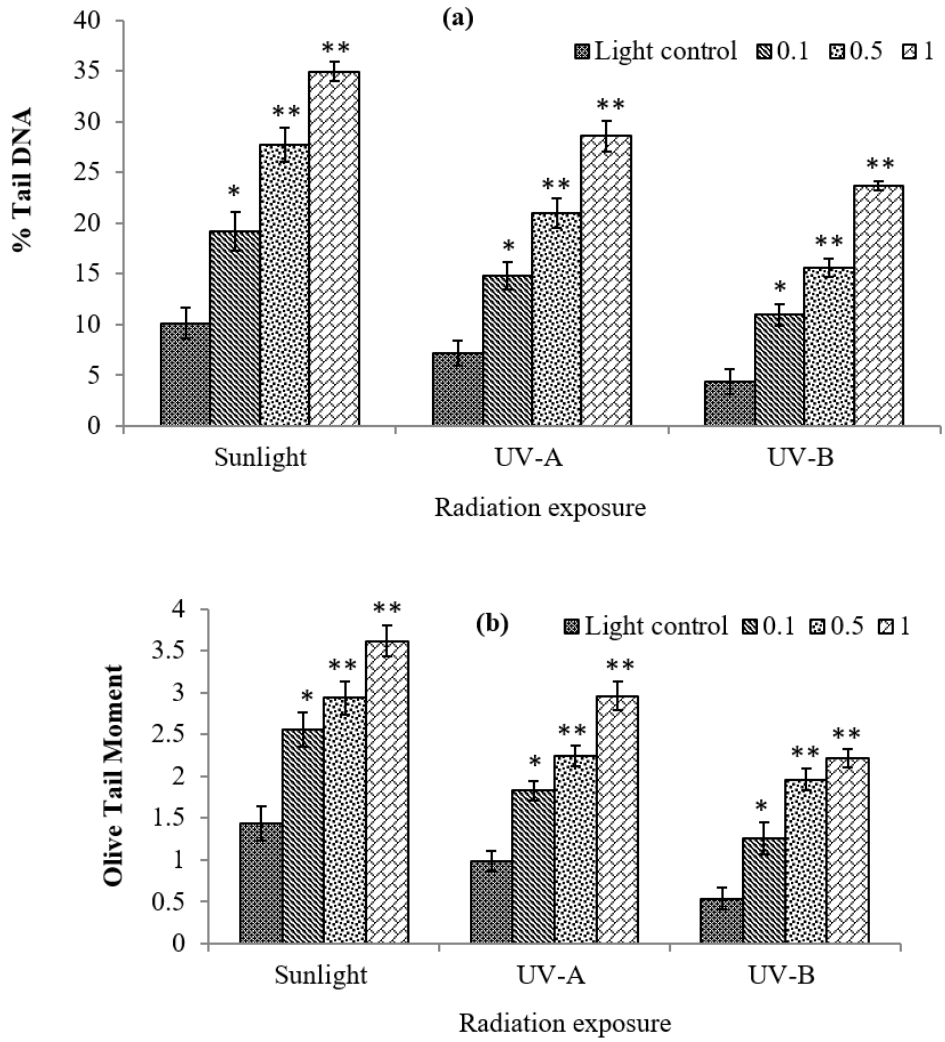

Fig. 6 DNA damage in keratinocytes after exposure of pyrene under Sunlight (30 min), UV-A (2.16 J/cm^2), and UV-B (0.72 J/cm^2) exposure **(a)** % Tail DNA **(b)** Olive tail moment. Values presented are mean of three observations ± SE. (*p<0.05 or **p<0.01- as compared to Light control).

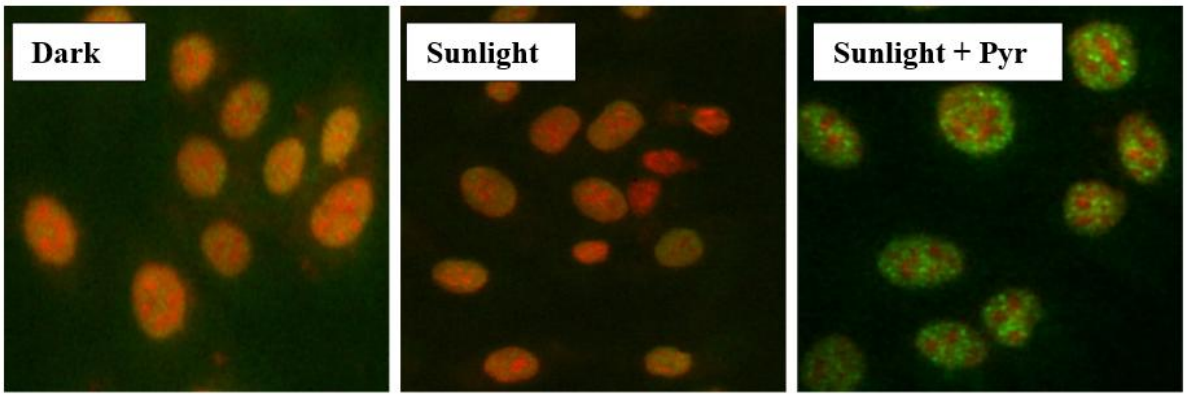

Fig. 7 Genotoxic evaluation of pyrene (1µg/ml) under sunlight (30 min) exposure. Maximum CPDs formation was under joint exposure of pyrene under sunlight exposure. No significant CPDs were detected under sunlight exposure alone and dark control cells.

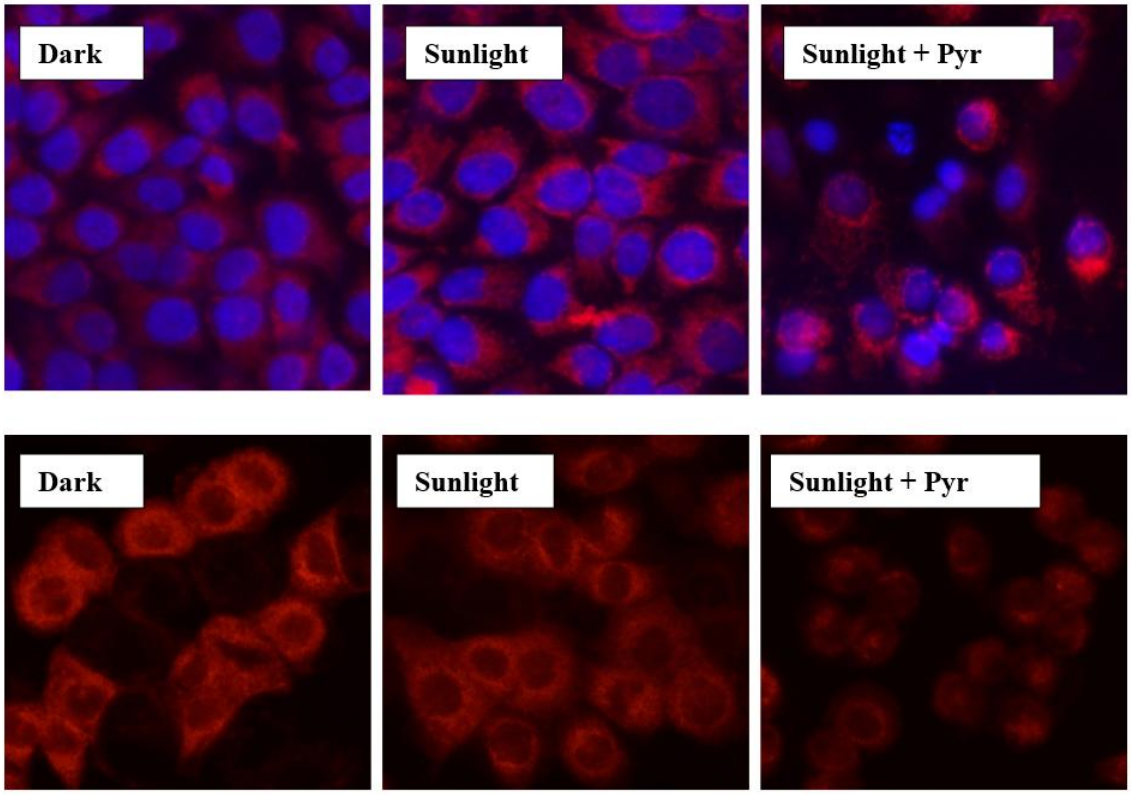

Fig. 8 Analysis of Mitochondrial membrane and its relation with DNA damage after treatment with pyrene under sunlight exposure. Fluorescence micrographs of keratinocytes showing decrease in mitochondrial membrane potential after treatment of pyrene under sunlight (30 min) exposure. MitoRed and DAPI double staining showed the relation of mitochondrial depolarization and DNA damage as well as Rhodamine staining to assess mitochondrial membrane potential.

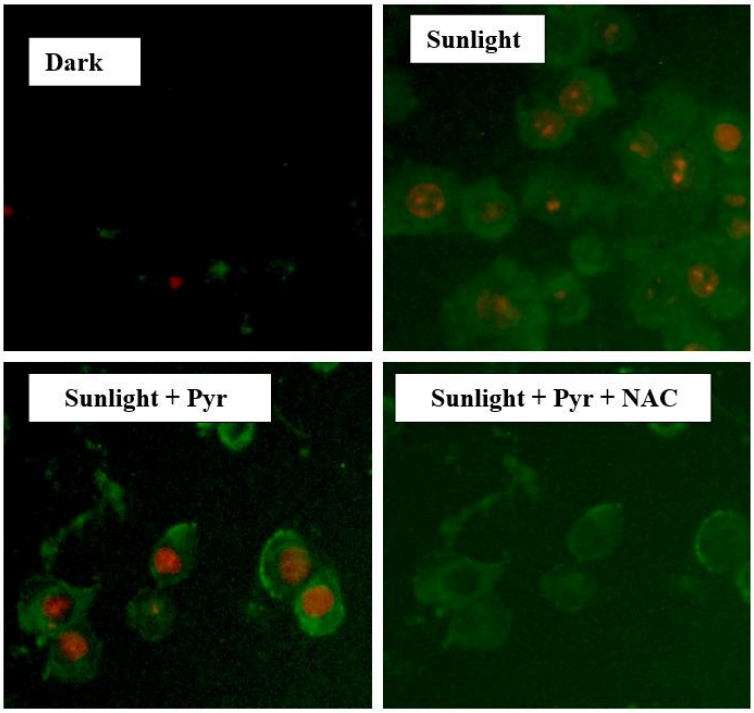

Fig. 9 Analysis of apoptotic cell death. Fluorescence images of Annexin V/PI double staining, showing maximum apoptotic cells after treatment with pyrene (1 µg/ml) under sunlight (30 min) exposure. There was no significant apoptotic cells detected in dark control and sunlight exposure alone. NAC (10 µM) reduced the apoptotic cell death in keratinocytes after treatment with pyrene (1 µgml) under sunlight (30 min) exposure.

III. Discussion

Pyrene is an ubiquitous environmental pollutant and also reported in human diet (Sivaswamy et.al., 1990), it always exposed to sunlight due to its environmental presence. In the present study we addressed the effect of natural sunlight on pyrene treated keratinocytes. Pyrene showed maximum absorption (λmax) in UV-A (334 nm). Our photomodification study showed that pyrene is stable upto 4 hr of sunlight exposure.

Pyrene under sunlight/UV-R exposure generates $^1O_2$ and $O_2^{\bullet-}$ through type-I and type-II photodynamic reactions. Maximum generation of ROS was detected under sunlight exposure followed by UV-A and UV-B exposures. There was no significant generation of either $^1O_2$ and $O_2^{\bullet-}$ detected under dark control and sunlight/ UV-R exposure alone. Generation of $^1O_2$ and $O_2^{\bullet-}$ was confirmed by specific quenchers NaN_3 and SOD, respectively. In addition to $^1O_2$ and $O_2^{\bullet-}$photosensitized pyrene also generates $^{\bullet}OH$ under sunlight/UV-R exposure, which was confirmed through their specific quenchers such as mannitol and sodium benzoate.

Our previous study suggests that anthracene generates ROS like $^1O_2$ and $O_2^{\bullet-}$ through type-I and type-II pathway under sunlight/UV-R exposure (Mujtaba et.al., 2011). Intracellular ROS generationwere detected through DCF-fluorescence intensity and was maximum at 1 µg/ml pyrene concentration under sunlight followed by UV-A and UV-B exposures. There was no significant ROS generation was detected in dark control cells. Generation of ROS was also seen under sunlight/UV-R exposure alone but along with pyrene, the generation was significantly higher. To confirm the intracellular ROS generation, NAC was used as a quencher, which reduced the DCF intensity significantly.

ROS can cause severe stress in cells, leading to the oxidation of cellular components including lipids, proteins and DNA, and in some cases the cleavage of DNA (Toyooka et.al., 2004). Pyrene induced ROS mediated single strand breakage of DNA in keratinocytes under sunlight/UV-R exposure. Maximum DNA damage was seen under sunlight exposure.

Cyclobutane pyrimidine dimmers (CPDs) formation was also detected in keratinocytes after treatment with pyrene under sunlight exporue. Pyrene did not significantly induced CPDs formation under dark control and sunlight exposure alone.

Pyrene reduced keratinocytes viability significantly under sunlight/ UV-R exposure. Maximum reduction in cell viability was seen under sunlight followed by UV-A and UV-B exposures. There was no significant reduction in viability in dark control cells. Hence, we propose that photosensitized pyrene generates ROS like $^1O_2$ and $O_2^{\bullet-}$ which were responsible for single strand DNA breakage and CPDs formation and finally reduction in cell viability. Benzo(a)pyrene induced intracellular ROS generation, DNA damage and finally cell death in perfused lung cells of mice *in vitro* (Mukherjee et.al., 2013).

To further confirm the apoptotic cell death PS translocation were detected through annexin-V and PI staining. Maximum apoptotic cells were detected under joint exposure of pyrene and sunlight exposure. There was no significant apoptotic cells were seen in dark control and sunlight exposure alone. Previous results suggest that tBHP induced apoptotic cell death in both N2A and SH-SY5Y cells and were detected through Annexin-V and PI double staining (Zhao et.al., 2005). To elucidate the ROS mediated DNA damage induced apoptotic cell death, NAC was used as a quencher to prevent ROS mediated apoptosis. Pyrene under sunlight exposure reduced apoptotic cells when treated with NAC which quenches the ROS generation in keratinocytes.

IV. Conclusion

The study conclude that the pyrene is photostable under natural sunlight exposure. Pyrene generates ROS mediated apoptosis in keratinocytes through DNA damage. Hence, it is important to look the environmental concentrations and its toxicity impact on human beings due to stability of pyrene in the environment.

References

[1]. Toyooka T. and Y. Ibuki (2007). DNA damage induced by coexposure to PAHs and light. Environmental Toxicology and Pharmacology, 23; 256-263.
[2]. Yan J., L. Wang, P. P. Fu and H. Yu (2004). Photomutagenicity of 16 polycyclic aromatic hydrocarbons from the US EPA priority pollutant list. Mutat. Res., 557; 99.
[3]. Kochany J., R. J. Maguire (1994). Abiotic transformations of polynuclear aromatic hydrocarbons and polynuclear aromatic nitrogen heterocycles in aquatic environments. Sci. Total Environ., 144; 17.
[4]. Mujtaba S. F., A. Dwivedi, M. K. R. Mudiam, D. Ali, N. Yadav, R. S. Ray (2011). Production of ROS by photosensitized anthracene under sunlight and UV-R at ambient environmental intensities, Photochem. and Photobiol., 87; 1067-1076.
[5]. Teranishi M., T. Toyooka, T. Ohura, S. Masuda and Y. Ibuki (2010). Benzo(a)pyrene exposed to solar-simulated light inhibits apoptosis and augments carcinogenicity. Chemico-Biological Interactions., 185; 4-11.
[6]. Ingram A. J. (1992). Review of chemical and UV light- induced melanomas in experimental animals in relation to human melanoma incidence. J. Appl. Toxicol. 12; 39.
[7]. Pierce A. J., J. M. Stark, F. D. Araujo, M. E. Moynahan , M. Berwick, and M. Jasin (2001). Double-strand breaks and tumorigenesis. Trends Cell Biol. 11; S52-S59.
[8]. Sigounas G., J. W. Hairr, C. D. Cooke, J. R. Owen, A. S. Asch, D. A. Weidner and J. E. Wiley (2010). Role of benzo(a)pyrene in generation of clustered DNA damage in human breast tissue. Free Radical Biology and Medicine, 49; 77-87.

[9]. Sivaswamy S. N., Balachandran, B., Sivaramkrishnan, V.M., (1990). Polynuclear aromatic hydrocarbons in South Indian deit. Curr. Sci., 59; 9.
[10]. Mukherjee A., N. Boujedaini, A. R. K.Bukhsh (2013). Homeopathic thuja 30C ameliorates benzo(a)pyrene- induced DNA damage, stress and viability of perfused lung cells of mice in vitro. Journal of Integrative Medicine, 11(6); 397-404.
[11]. Amy C., Long, C. M.H. Colitz, and J.A. Bomser (2004). Apoptotic and necrotic mechanisms of stress induced human lens epithelial cell death. Experimental Biology and Medicine, 229; 1072-1080.
[12]. Toyooka T., Ibuki, Y., Koike, M., Ohashi, N., Takahashi, S., and Goto, R. (2004). Coexposure to benzo[a]pyrene plus UV-A induced DNA double strand breaks: visualization of Ku assembly in the nucleus having DNA lesions. Biochem. Biophys. Res. Commun., 322 (2); 631-636.

Graphical abstract of Pyrene phototoxicity.